Measurement of the angular distribution of neutrons scattered from deuterium below 3 MeV

Elisa Pirovano[1,*], *Ralf* Nolte[1], *Markus* Nyman[2], and *Arjan* Plompen[2]

[1]Physikalisch-Technische Bundesanstalt, Bundesallee 100, 38116 Braunschweig, Germany
[2]European Commission, Joint Research Centre, Retieseweg 111, 2440 Geel, Belgium

Abstract. The differential cross section of neutron scattering on deuterium was investigated in the energy range from 400 keV to 2.5 MeV using the recoil detection method, irradiating with monoenergetic neutrons a proportional counter filled with deuterated gases. Comparing simulations of the transport of neutrons and recoil nuclei in the detector to the experimental pulse-height distribution, it was possible to establish a procedure for the determination of the coefficients of the Legendre expansion of the n-d angular distribution.

1 Introduction

Accurate experimental data describing elastic scattering of neutrons on deuterium are of interest for fundamental research in the field of quantum-mechanical few-body systems, and practical applications in metrology, detector development, and for the safe operation of heavy-water moderated critical systems. Below 3 MeV of incident energy, however, the available measurements of neutron angular distributions are scarce and partially discrepant, especially at backward angles [1]. Issues were documented also with the evaluated nuclear data libraries, which were found to produce inconsistent results when modelling benchmark experiments for heavy-water moderated critical assemblies [2]. This called for a re-evaluation of the angular distribution of n-d scattering below 1 MeV [3], and several measurement campaigns were started to solve the discrepancies in the experimental database (e.g. [4–6]).

The measurement presented here aims at the reconstruction of the neutron angular distributions over a large angular range. It was performed at the PTB Ion Accelerator Facility (PIAF) [7], where monoenergetic neutrons in the energy range from 400 keV to 2.5 MeV were produced to irradiate a proportional counter filled with mixtures of deuterated gases. The counter served as target for the incident neutrons and detector for the recoil deuterons simultaneously, according to the concept originally presented in [4]. The recoil detection method was extended to higher incident neutron energies by adopting different gas and pressure combinations, reducing the range of recoil deuterons and so limiting their escape from the detector sensitive volume. A new analysis procedure was also developed, which allowed the determination of the angular-distribution Legendre-expansion coefficients from the comparison of simulations to experimental data.

*e-mail: elisa.pirovano@ptb.de

2 Experimental setup

The measurements were carried out in the low scatter hall of PIAF, where monoenergetic neutron fields were produced in open geometry using the ^{7}Li(p,n)^{7}Be and ^{3}H(p,n)^{3}He reactions. A metallic lithium target was employed (instead of the more common LiF target) in order to minimise the photon contamination of the neutron field. The detector was placed at 1 m distance from the neutron producing target, at 0 degrees relative to the direction of the ion beam. At this position, the neutron energies ranged from about 400 keV to 2.5 MeV: the nominal mean neutron energy incident on the counter and the energy spread are listed in Table 1.

The counter used for the experiment, P2, is a recoil proton proportional counter routinely used for neutron fluence measurements (details can be found in [4]). In this case, P2 was operated with: a D_2/CD_4 mixture at a pressure of 1000 hPa (96.5% in volume of D_2 and 3.5% of CD_4, for incident neutron energies from 400 keV to 620 keV), deuterated propane (C_3D_8) at 600 hPa (for energies between 500 keV and 1.25 MeV), and C_3D_8 at 1000 hPa (for energies above 1.5 MeV). Propane has a higher stopping power than D_2, which makes it more suitable for measurements at higher energies: the shorter range of the recoil deuterons reduces the probability of incomplete energy deposition events due to particle escaping the sensitive volume of the detector. This however comes with the disadvantage of having a higher carbon content. The photon-induced events were subtracted using the rise-time discrimination technique, which is thoroughly described in [4]. To subtract the contribution of room-return neutrons, for each incident energy data were taken with and without a shadow cone (300 mm of polyethylene and 200 mm of iron).

For elastic scattering, the energy of the recoil nucleus in the laboratory system is related to the neutron scattering angle in the centre-of-mass reference system, and the

Table 1. Summary of the measurement runs. For each neutron producing reaction, and each neutron producing target, a list with the nominal mean energy E_n and energy spread ΔE_n of the neutron field at the counter position is provided. Each ($E_n \pm \Delta E_n/2$) combination refers to a separate run.

Reaction	Target	List of ($E_n \pm \Delta E_n/2$)
^{7}Li(p,n)^{7}Be	metallic Li, 100 µg/cm^2	(385±8) keV; (495±7) keV; (620±7) keV; (748±7) keV; (868±6) keV.
^{3}H(p,n)^{3}He	T/Ti, 500 µg/cm^2	(864±31) keV; (1.00±0.03) MeV; (1.25±0.03) MeV; (1.50±0.03) MeV.
^{3}H(p,n)^{3}He	T/Ti, 955 µg/cm^2	(2.00±0.04) MeV; (2.50±0.04) MeV.

recoil energy distribution is proportional to the differential cross section. The measured distributions therefore mainly reflect the shape of the angular distribution of n-d scattering. With C_3D_8, carbon also significantly contributes to the detector response: this results in a two-step distribution (figures 1(b) and 1(c)), as compared to the one-step distribution obtained with D_2/CD_4 (figure 1(a)), where carbon is negligible.

Real detectors, however, do not provide a direct measurement of the recoil energy distribution, but of the ionisation in the counting gas, which is related to the deposited energy. Therefore, instrumental effects such as incomplete energy deposition in the sensitive volume or an energy dependence of the mean energy W required to produce an ion pair were included in a realistic Monte Carlo simulation of the pulse-height distributions produced by the proportional counter, folded with a Gaussian response function of constant relative width to model the pulse-height resolution of the instrument [4].

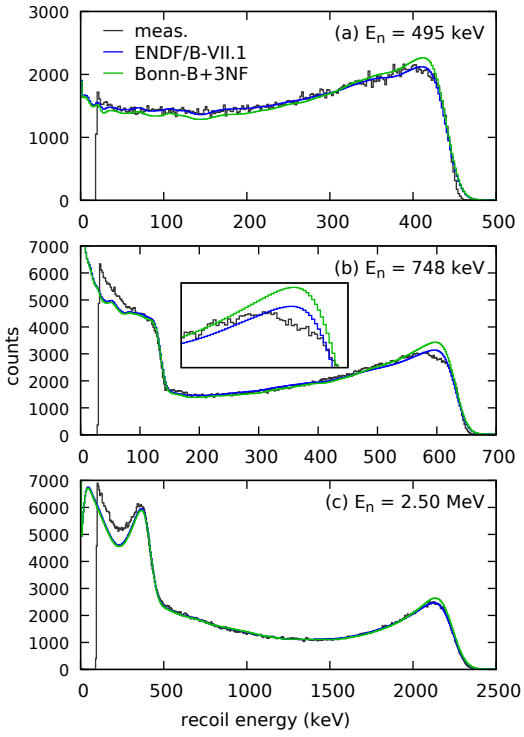

Figure 1. Histograms showing the recoil deuteron energy distribution for selected incident neutron energies E_n. The measurements ("meas.") are compared to the results of the Monte Carlo model using, for n-d scattering, the differential cross section from the ENDF/B-VII.1 library or the theoretical calculation of Canton *et al.* ("Bonn-B+3NF") [8].

3 Comparison with current libraries

For each neutron energy, the Monte Carlo simulations were repeated using different models for the n-d differential cross section, shown in figure 2. Golak *et al.* [9] ("N3LO chiral forces" in the figure) performed an *ab initio* calculation applying the effective-field chiral perturbation theory and derived the three-nucleon forces ("3NF") to the fourth order of the chiral expansion (next-to-next-to-next-to the leading order, N3LO). Canton *et al.* [8] combined the Bonn-B nucleon-nucleon potential with the 3NF obtained considering the irreducible effects generated by the one-pion-exchange mechanism, and computed the differential cross section with and without three-body forces ("Bonn-B+3NF" and "Bonn-B", respectively). The ENDF/B-VII.1 library [10] is the result of a coupled-channels R-matrix analysis. The angular distribution of ENDF/B-VIII.0 [11] is taken from the JEFF-3.3 li-

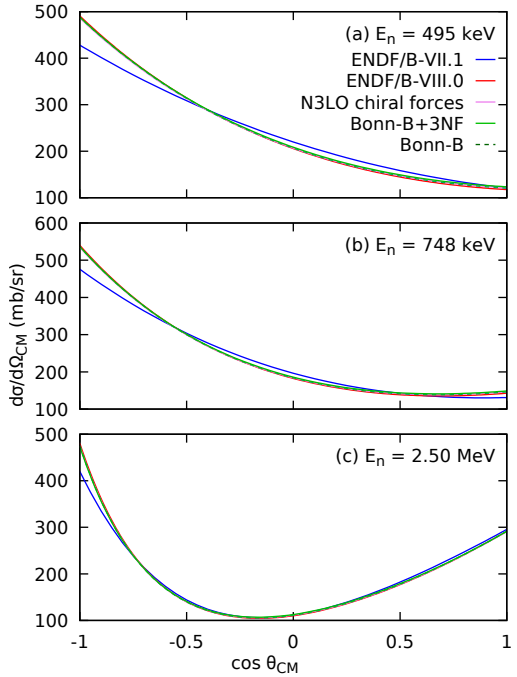

Figure 2. Differential cross section $d\sigma/d\Omega_{CM}$ as a function of the neutron scattering angle in the centre-of-mass system θ_{CM} for three of the measured incident neutron energies E_n. The description of models and evaluations producing these results can be found in section 3.

brary [12], in which the n-d reaction is considered as a three-particle problem for nucleons interacting via pairwise potentials and is solved by means of the Faddeev equations.

The different solutions of the three-body problem are so similar to each other that the corresponding lines in figure 2 (i.e., all but "ENDF/B-VII.1") are barely distinguishable. The same is also true for the calculation of Canton with and without the three-body potential, as the 3NF effects on angular distributions are negligible below 30 MeV of incident neutron energy. For this reason, the recoil counter response was simulated considering the ENDF/B-VII.1 library and the "Bonn-B+3NF" model only (see figure 1).

There are cases in which the Monte Carlo model does not account for the lower part of the recoil energy distribution, independently from the choice of the n-d differential cross section (e.g., below 100 keV in figure 1(b) and below 300 keV in figure 1(c)). This is caused by a residual photon contamination in the experimental data, and limits the analysis to the higher part of the recoil energy distribution and to large neutron scattering angles. This is a minor drawback, as we are mostly interested in the results at backward angles anyway.

The recoil distributions are generally better reproduced by the simulations based on the ENDF/B-VII.1 library rather than those using 3NF model. The "Bonn-B+3NF" model seems to overestimate the backward-forward asymmetry of the reaction, producing more counts in the recoil peak than observed. This is surprising, as other recent measurements [6] and heavy-water reactor benchmark modelling [13] favour evaluations based on three-body theories instead.

These results, however, are not conclusive. Both the ENDF/B-VII.1 evaluation and the 3NF model do not reproduce the shape of the recoil peak: in figure 1(b), for example, the experimental peak is clearly broader than in the simulations. This issue was noticed at all neutron energies, but to a lesser extent. Its shape cannot be recreated by adjusting the shape of the n-d differential cross section without completely distorting it; it is probably not a feature of n-d scattering. The fact that the discrepancies increase with the chronological order of the runs indicates a gradually intensifying disturbance: one possibility is that the neutron producing target material (i.e. lithium or tritium) diffused into the backing. Diffusion would in fact end up in a broader incident neutron energy distribution than that calculated from the nominal target thickness, and this would turn into a broader recoil peak too.

The neutron energy distribution was not measured during the experiment. In stable operation conditions it is not necessary as it can be accurately calculated using the dedicated Monte Carlo code TARGET [14], which simulates ion and neutron transport in the target assembly. Moreover, at the time of the experiment (right before the old Van de Graaf of PIAF was replaced with a tandem accelerator), setting up the pulsed beam needed for the time-of-flight technique would have been extremely time consuming. Due to the limited available beam time, it was therefore decided to measure only the average neutron energy with an ^{3}He proportional counter.

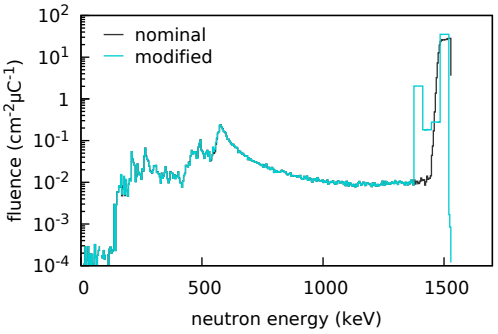

Figure 3. Energy distribution for the incident neutrons fluence per unit charge (protons hitting the tritium target) with 1.50 MeV average energy. The "nominal" distribution is the result of the TARGET code, while the "modified" distribution was deduced from the nominal in an iterative procedure comparing Monte Carlo simulations to the experimental pulse-height histogram.

To estimate how the neutron distribution would have to change in order to explain the discrepancies, the Monte Carlo code used to simulate the recoil counter response was modified to allow the use of the maximum-likelihood method to tune the initial input quantities iteratively, by comparison with the measured histograms. The incident energy distribution was then adjusted, while the n-d angular distribution was kept fixed to ENDF/B-VII.1.

In figure 3, the initial distribution, computed with the TARGET code for the average neutron energy of 1.50 MeV, is plotted against the result of this procedure. The nominal distribution is characterized by a narrow, almost flat peak, whose width depends mainly on the target thickness, and a tail (2.5% of the total fluence in this case) of neutrons scattered in the target structural elements. The adjusted distribution displays a broader peak, and it includes a dip in correspondence to the separation surface between backing and target, possibly being a sign of non-continuous diffusion.

4 Determination of the neutron angular distribution

Adjusting the energy distribution improved the agreement for both ENDF/B-VII.1 and the 3NF-based simulations, supporting the idea of the target diffusing into the backing. However, it also introduced a bias in favour of the library used for n-d scattering during the adjustments. A more rigorous approach would be repeating the experiment, including an independent measurement of the neutron energy distribution. Before that, it is interesting to test if this kind of data could be used for more than the comparison with the existing libraries, e.g. if they could be used to determine of the Legendre coefficients of the neutron angular distribution.

To do it, the "pseudo-Legendre components" of the pulse-height distribution were calculated up to the 4th order. The recoil counter model was employed once again:

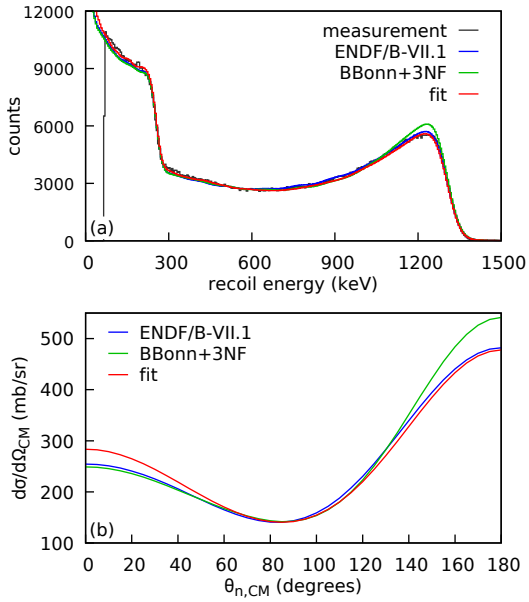

Figure 4. Result of the fit of the pseudo-Legendre components for 1.50 MeV incident neutrons. In figure (a) the fit is compared to the experimental pulse-height histogram and simulations with the ENDF/B-VII.1 evaluation and the theoretical calculation of Canton *et al.*, in figure (b) the corresponding differential cross sections are shown.

this time, the detector response was calculated considering fictitious n-d angular distributions corresponding each time to one Legendre polynomial of given order, and, to generally improve the agreement with the data, the "modified distribution" of figure 3 was used as input for the incident energy distribution. The linear combination of the pseudo-component was fitted to the experimental histogram corrected for n-C and multiple scattering. The resulting coefficients were used then to build the Legendre expansion of the neutron angular distribution. The results for 1.50 MeV neutrons are shown in figure 4(a) for the pulse-height histogram, and in figure 4(b) for the differential cross section.

At forward angles (angles smaller than 60 degrees in the centre-of-mass system) the cross section is overestimated because the fit includes the photon events that could not be subtracted from the experimental histogram. At backward angles, the ENDF/B-VII.1 evaluations is still the closest to the data, but that could also be an effect of having used ENDF/B-VII.1 in the energy adjustments.

Considering the large uncertainties on the incident energy, this analysis was performed only at 1.50 MeV as proof of concept. With better control over the systematic uncertainties, the collected statistics would have been enough to produce results able to discriminate between calculations and evaluations at backward angles. At these angles, in the energy range from 400 keV to 2.5 MeV, the discrepancies go to up 10% between different models and 40% with the available experimental data. A new improved measurement could therefore produce valuable results.

5 Conclusions

A new measurement of the differential cross section of n-d scattering was carried out at PIAF, where a recoil counter filled with deuterated gases was irradiated with monoenergetic neutrons from 400 keV to 2.5 MeV.

The experimental pulse-height distributions were corrected for room-return neutrons and photons. A dedicated Monte Carlo model was developed for the simulation of the transport of neutron and recoil ions in the sensitive volume of the detector and was used to analyse the counter response. The Legendre coefficients of the n-d scattering angular distribution could be determined by fitting simulations to experimental data.

The collected statistics would have allowed to produce precise results, their accuracy however ended up to be significantly limited by the lack of direct measurements of the incident neutrons energy distribution, owing to beam-time limitations.

Building on this experience, and taking advantage of the recent upgrade of PIAF, the intention is to repeat the measurement with pulsed beam, as that would allow the use the time-of-flight technique for the neutron energy determination and to keep the systematic uncertainties under control.

References

[1] L.W. Townsend, AECL Final Technical Report Purchase Order 217739 (2006)
[2] K.S. Kozier, in *PHYSOR 2006 Topical Meeting* (ANS, Vancouver, BC, 2006), pp. 2123–2132
[3] OECD NEA, *HPRL*, available at www.oecd-nea.org/dbdata/hprl/
[4] R. Nolte et al., in *ERINDA Workshop* (CERN, Geneva, Switzerland, 2013), pp. 187–195, CERN-Proceedings-2014-002
[5] N. Nankov et al., Nucl. Data Sheets **119**, 98 (2014)
[6] E. Pirovano et al., Phys. Rev. C **95**, 024601 (2017)
[7] H. Brede et al., Nucl. Instrum. Methods **169**, 349 (1980)
[8] L. Canton et al., Eur. Phys. J. A **14**, 225 (2002)
[9] J. Golak et al., Eur. Phys. J. A **50**, 177 (2014)
[10] M.B. Chadwick et al., Nucl. Data Sheets **112**, 2887 (2011)
[11] D. Brown et al., Nucl. Data Sheets **148**, 1 (2018)
[12] OECD NEA, *JEFF-3.3*, available at www.oecd-nea.org/dbdata/jeff/jeff33/
[13] B. Morillon et al., Ann. Nucl. Energy **54**, 167 (2013)
[14] D. Schlegel, Tech. Rep. PTB-6.42-05-2, PTB (2005)